COO-2679-13

LOW ENERGY PLANES FOR TILT GRAIN BOUNDARIES IN GOLD

by

P.J. Goodhew*, T.Y. Tan†, and R.W. Balluffi

Department of Materials Science and Engineering
and the Materials Science Center
Cornell University, Ithaca, N.Y. 14853

May 1977
Cornell University
Ithaca, N.Y. 14853

Report #2840
Issued by
The Materials Science Center

* Permanent address: Department of Metallurgy & Materials Technology, University of Surrey, Guildford, GU2 5XH, England.

† Now at: I.B.M., Essex Junction, Vermont 05452, U.S.A.

DISCLAIMER

ABSTRACT

Thin film bicrystals of gold were annealed to create a large variety of grain boundaries of controlled crystal misorientation. The faceting of these boundaries has been studied and some low energy boundary planes identified. Tilt boundaries with a <110> misorientation axis have been found to facet more readily than those with a <100> axis. The results have been considered in terms of O-lattices and coincident site lattices but neither of these approaches is able to explain all the observations. Consequently no simple and general criteria, based on geometrical considerations, have been found for the occurrence of grain boundary planes of low energy.

A further set of observations relates to the dissociation of some specific high angle grain boundaries into a twin and another low energy boundary. Boundaries with a $\Sigma 33$ coincidence site lattice relationship frequently appear to be characterized by a relatively low energy.

*****

1. INTRODUCTION

It is well established that the structure and energy of a grain boundary depend, not only on the crystal misorientation between the contiguous grains, but also on the orientation of the particular plane adopted locally by the boundary (1) and possibly on the temperature (2). Several geometrical models have been proposed which might account for the occurrence of particular misorientations and boundary planes which have a low energy associated with them (3-10). Those models based on the concepts of the coincidence site lattice (CSL) (3,4,5) near-coincidence site lattice (NCSL) (6) and structural unit (7,8) predict certain special misorientations which might be expected to contain low energy boundary planes because of a high degree of fit between the atoms in both grains. The planar matching model (9,10) on the other hand, although it predicts special misorientations, would not explain the occurrence of low energy boundary planes associated with those misorientations.

The faceting of a grain boundary implies that low energy boundary planes do exist and such faceting has been observed in several systems on both macroscopic (11,12) and microscopic (13,14,15) scales.

An early criterion for the occurrence of facets in boundaries near a high density CSL misorientation was simply that a boundary passing through a plane of the CSL possessing a high planar coincidence site density (PCSD*) would have a relatively low energy configuration (4), presumably because of the relatively short (two-dimensional) periodicity of the boundary and hence the absence of long range distortions. The most frequently quoted example is the first order twin system ($\Sigma 3$ in the conventional CSL nomenclature) which very readily facets onto a common {111} and a common {112} plane (16), both of which have a high PCSD (2.31 and 0.82 respectively). However, because of the special nature of the {111} twin facet, in which no atom is appreciably displaced from a normal lattice site, this system may not display

---

*PCSD is defined as the number of coincident sites per area a^2 of the boundary plane, where a is the lattice parameter.

typical faceting behaviour and it is probably unwise to draw general conclusions from such observations. The only other reported observation of faceting of a boundary between two high density-coincidence-related grains is that of Wagner, et al, (13). They observed the decomposition of one particular Σ5 tilt boundary lying in a plane of low PCSD (0.28) into two facets lying in planes of much higher PCSD (0.89 and 0.63). On the other hand, boundaries of relatively low PCSD are also frequently observed, such as the $\{113\}_1$ vs. $\{335\}_2$* boundary in Cu (17); the $\{117\}_1$ vs. $\{551\}_2$ boundary in Al (18,19, PCSD = 0.56); the $\{531\}_1$ vs. $\{531\}_2$ boundary, the $\{110\}$, vs. $\{110\}_2$ boundary, and the $\{335\}_1$ vs. $\{7, 13, 13\}_2$ boundary in a Ni-Fe alloy (20); the $\{5, 5, 13\}_1$ vs. $\{7, 7, 11\}_2$ boundary and the $\{110\}_1$ vs. $\{110\}_2$ boundary in an austenitic steel (21). It appears that the boundary having the highest PCSD (0.77) in the Σ9 system**, $\{111\}_1$ vs. $\{115\}_2$, has also been observed in Cu (22), and in steel (21). Vaughan (21) has shown, however, that this boundary is really composed of boundaries of two Σ3 systems on a microscopic scale.

Strong faceting on a macroscopic scale has been observed in both silver (12) and zinc (11). In neither set of experiments were any of the boundaries close to a high density CSL misorientation. However, it was possible to interpret the facet planes in terms of slightly strained structural units of relatively short periodicity in the boundary. Neither set of observations lends direct support to the PCSD criterion for low boundary energy, although the authors' interpretations imply that a relatively high density of locally low-energy atomic configurations occur in the special boundary planes. This is as far as one can go towards a PCSD criterion in the absence of a significant density of coincidence sites.

A further set of observations which has a bearing on faceting is the recent study by field ion microscopy of grain boundary topography in tungsten (23). The significant conclusion was that although two (possibly three) of the boundaries were close to a high density CSL misorientation, and all the boundaries showed essentially planar areas, only one of the planar

---

*In this nomenclature a $\{hkl\}_1$ plane in crystal 1 and a $\{hkl\}_2$ plane in crystal 2 lie parallel to the boundary.

**The Σ9 system has often been referred to as the second order twin system.

segments occupied a plane of high PCSD. This single example was a {111} twin plane, and for the reasons mentioned above this gives very little weight to the PCSD criterion.

In view of the sparsity and inconclusiveness of existing experimental evidence, particularly from boundaries which are very close to a high density CSL misorientation, the present authors decided to study faceting behaviour in tilt boundaries of well-controlled misorientation in an attempt to establish more clearly possible criteria for the occurrence of facets.

2. EXPERIMENTAL TECHNIQUE

2.1 Specimen Preparation and Observation

All our observations were made on thin gold bicrystals using a JEM-200 or Siemens Elmiskop 102 microscope. The bicrystal specimens were made in two ways: the majority of specimens contained a grain boundary generated by welding together two single crystal ({100} or {110}) films at the chosen angular misorientation. This technique has been fully described elsewhere (24). The bicrystal films were then annealed until the boundary (originally in the midplane of the thin film) had migrated to create many "island" grains with boundaries perpendicular to the foil (25) (Figure 1). This technique was used to generate tilt boundaries with misorientations very close to those of the Σ3,5,9,11,13,17,19,25 and 33 coincidence site lattices (CSLs) as well as many less special high angle boundaries.

In addition, one set of specimens was created by deposition of gold onto a cleaved NaCl substrate held at a lower temperature than is necessary for epitaxial growth. This gives rise to a quadruply positioned gold film with (111) grains separated by Σ3 twin boundaries (16) and enables the {211} twin boundaries to be examined.

2.2 Micrograph Interpretation

Observations were only recorded of boundaries which were perpendicular to the foil surface and viewed exactly end-on. The local misorientation across each boundary and the inclination of the boundary could then be measured directly from the diffraction

pattern from a selected area which spanned the boundary.

In those cases where straight facets were immediately evident they could be related to within $\pm 1^{o}$ to the orientations of the two grains. In cases where facets were not obvious, micrographs were recorded of small closed loops of boundary ("island" grains) and enlarged prints of these areas were analysed using a computer routine which calculated the proportion of the boundary lying in each inclination. This is an image analysis function not readily available on conventional image analysers; details of the routine can be obtained from P.J.Goodhew. The output is presented as a polar histogram showing the proportion of the total boundary in each inclination sector (e.g. Figure 4).

3. RESULTS

Our observations fall into three fairly distinct categories, particularly as regards their interpretation, so we will consider the $\Sigma 3$ boundaries, the <100> tilt boundaries and the <110> tilt boundaries separately.

3.1 First Order Twin ($\Sigma 3$) Boundaries

The welded bicrystals in which the $\Sigma 3$ boundary was generated by a 70.5^{o} rotation about <110> show a strongly faceted island structure which is typified by Figure 2. As might be expected the main facet is the coherent twin boundary on {111}. The shorter, and sometimes less straight, facets are in general perpendicular to the major facets and are clearly the incoherent {112} twin boundaries. Observation of the quadruply positioned films which contain many 60^{o} <111> boundaries confirms that all three of the {112} twins are present as facets in this section of the $\Sigma 3$ CSL (e.g. Figure 3). The coherent twin is not present in this system since it would be parallel to the foil plane and is unlikely to grow in such a high energy configuration.

3.2 <100> Tilt Boundaries

Special boundaries with this misorientation axis include $\Sigma 5,13,17$ and 25. Boundaries with misorientations within 0.5^{o} of these CSLs and other high angle boundaries chosen to be as far as possible from a high density CSL (low Σ) misorientation were

.../6.

examined along with a number of low angle boundaries. No example of immediately obvious faceting was observed. At least ten micrographs from each specimen were then computer analysed to determine whether any boundary inclinations were, on average, preferred. A typical polar histogram is shown in Figure 4 for boundaries of 7.5^{o} misorientation, from which it can be seen that the inclinations for these boundaries are not randomly distributed but that an inclination near the mean [011] of the two grains is preferred. In general the preference for the mean [011] inclination was found to be quite strong for boundaries of low misorientation angle (θ) and became less marked as the angle increased. For boundaries of $\theta > 30^{o}$ no preference for the mean [011] inclination could be detected.

In addition, for many boundaries, more especially those with higher θ, there is some evidence of preferred inclinations parallel to a <100> in each grain. Other work in our laboratory has shown, by means of hot stage observations of the boundary migration processes which lead to this specimen geometry, that these inclinations are introduced in the early stages of boundary migration (26). They are probably related to features in the single crystal films which are responsible for the heterogeneous nucleation of the breakthrough process shown in Figure 1.

We have considered, in two earlier papers (25,26) the extent to which the tilt boundary configurations which we observe reflect the equilibrium situation. Clearly the island grain is in any case merely a metastable configuration: however, we have no evidence that the facets and preferred planes which we have seen were developed by the preferential migration of specific boundary planes.

3.3 <110> Tilt Boundaries

CSL boundaries with a <110> misorientation axis include Σ3,9,11, 17,19 and 33. More than twnety boundaries with misorientations in the range 0^{o} to 90^{o} were examined and in most cases faceted island grains were found (e.g. Figure 5). An overall summary of the facet observations is given in Table 1. The facets are described in terms of the mean direction in the surface of the two crystals along which they lie, since this often leads to a particularly simple description which brings out similarities among the facets. Because the two crystals are related by a simple rotation about

an axis perpendicular to the specimen any direction lying in the specimen plane can be described as the bisector of two crystallographically equivalent directions, one in crystal 1 and the other in crystal 2. We call this bisector the mean direction and, for example, refer to the smallest bisector of $[111]_1$ and $[111]_2$ as $[111]_{mean}$. Where no low index mean direction is indicated the facet is described by its angle from $[001]_{mean}$.

For every type of boundary pairs of facets were found symmetrically disposed about $[001]_{mean}$ (e.g. Figure 6). One noteworthy aspect of the observations is that in the vast majority of cases the faceting was along low index mean directions. The possible significance of these directions is discussed in the next section.

A further observation was the occurrence of twinning within the island grains (Figures 7,8,9). This was observed most frequently in boundaries in the misorientation ranges $37^o < \theta < 41^o$, $49^o < \theta < 54^o$ and $\theta \approx 90^o$. Since in each case the twinning of a grain implies the replacement of a section of the grain boundary (misorientation θ_1) with a twin boundary ($\Sigma 3$, $\theta_3 = 70.53^o$) and a second boundary (misorientation $\theta_2 = \theta_1 \pm \theta_3$) we refer to this, in Table 1 and elsewhere, as "boundary dissociation". It is a consequence of the geometry of CSLs that at a triple point the Σ value of the third boundary is a multiple or submultiple of the Σ values of the other two boundaries. Thus for instance in the dissociation of the $\Sigma 9$ boundary into two $\Sigma 3$ boundaries 3X3=9. The mechanism and energetics of boundary dissociation are discussed in section 4.

4. DISCUSSION

4.1 First Order Twins

Our results confirm that the $\Sigma 3$ system facets strongly on the {111} coherent twin plane and, less markedly, on all the equivalent {112} incoherent twin planes. These two planes are those with the greatest density of coincident sites (PCSD): the coherent twin plane, in which all the atoms are coincident, has a PCSD of 2.31 while the {112} twin plane has a density of 0.82. It is evident from Figure 3 that when the specimen geometry permits both the {111}and {112} twins to lie perpendicular to the thin film, the islands facet in such a way that the majority of the boundary adopts

.../8.

the {111} facet. This is the behaviour to be expected if faceting occurs according to a Wulff-Herring criterion (27,28), and the {111} facet is of lower energy than the {112} facets. We should then be able to relate the relative areas of each facet (i.e. the shape of each island) to a polar Wulff plot showing the appropriate energy cusps. This is illustrated schematically in Figure 10 which has been constructed using values of 370 ergs/cm^2 for the energy of a high angle grain boundary in a random inclination (29,30) dropping to 25 ergs/cm^2 for the coherent twin (31). The other four cusps have then been assigned depths assuming that the cusp depth is linearly proportional to PCSD. Thus at the bottom of the coherent twin cusp PCSD = 2.31 while at the outer perimeter of the plot PCSD = 0. The four cusps shown then correspond to the inclinations of the next most dense CSL planes, having PCSDs of 0.82, 0.77, 0.67 and 0.56 in the Σ3 CSL. The equilibrium shape of faceted islands in this system can be determined graphically using the construction described by Herring (28). In the Σ3 system, because of the great depth of the cusp at the coherent twin plane, rectangular islands are predicted with only two types of facet. This clearly is in qualitative accord with our observations. The relative facet lengths are determined by the relative energies of the {111} and {112} facets. Using the PCSD criterion as illustrated in the figure, a {111} to {112} ratio of 9.2 to 1 is predicted. This is rather greater than our measured value of 3.35 to 1. If we use the only value for the incoherent {112} twin boundary energy quoted in the literature, 170 ergs/cm^2 (29) to determine the cusp depth instead of the PCSD value we find a ratio of 6.6 to 1, which is closer to the experimental value although still far enough away to cast doubt on the value of Chaudhari and Mader (29). We can of course use our experimental ratio to calculate an approximate incoherent {112} twin boundary energy from the many measured values of the coherent twin boundary energy. On this basis we expect the incoherent {112} energy to be near 85 ergs/cm^2.

4.2 <100> Tilt Boundaries

The absence of pronounced faceting in this system is in direct contrast with the behaviour of <110> tilt boundaries. Even in the Σ5 system (θ = 36.9°) where an observation of faceting has been made previously by Wagner, et al (13), we found no evidence of sharp facets even on the {210} twin plane with a PCSD of 0.89.

Of course, throughout the <100> tilt system the CSL unit cell is a body-centred square when projected onto (100) and is therefore more equi-axed than in the <110> system. Variations in the PCSD for low index CSL planes are therefore smaller. This, together with the high rotational symmetry of the system about [100] means that predictions based on PCSD indicate that faceted islands should be nearly equi-axed, as Figure 11 illustrates for the case of $\Sigma 5$.

The observed tendency for the low angle <100> tilt boundaries to prefer a $[011]_m$ inclination can be interpreted in terms of the O-lattice but not in terms of CSL concepts. For low angle boundaries the $[011]_m$ direction lies along the densest plane of the O-lattice*. The boundary therefore consists of a low density of identical lattice dislocations lying at the spacing of the O-lattice and possessing elementary lattice Burgers vectors. Such a boundary is therefore of relatively low energy. We have also observed a tendency of the boundaries to lie along $[011]_m$ during the earlier intermediate stages while the boundary is migrating to its position perpendicular to the film (26). Under these conditions the migration of the boundary occurs by the slip of consecutive screw dislocations to the specimen surface. These dislocations lie along $[011]_m$ and tend to constrain boundary segments to lie along this direction. As the misorientation angle increases the O-lattice spacing decreases and it becomes unrealistic to think of the boundary as being composed of individual dislocations. However, the formal O-lattice construction indicates that geometrically a similar situation exists although the 'dislocations' will be very close together. There is already electron diffraction evidence (32) that observable O-lattice relaxations occur for all <100> misorientations (i.e. up to 45^o) but it seems likely that the effect of these relaxations on the energy of the boundary is minimal above a misorientation of about 30^o. Thereafter the boundary apparently consists essentially of a plate of 'dislocation' core material (33) within which the atoms still adopt a very short period relaxation.

---

*As pointed out by Bollmann (41) a large number of O-lattices can be generated for each crystal misorientation. The physically important O-lattice in each case is that of largest spacing corresponding to the smallest value of det $|I-A^{-1}|$ where A = rotation matrix and I = identity matrix. The O-lattice referred to here is that generated by a simple rotation A around <100>.

Our results do not encourage the interpretation of faceting in terms of the CSLs, since we always see (for $\theta<30^{o}$) a preference for the $<011>_m$ boundary inclination while the densest CSL plane is fluctuating between $<011>_m$ (for Σ5 and 13) and $<010>_m$ (for Σ17).

A further conceivable approach to understanding the behaviour of the <100> boundaries may be in terms of planar matching. Clearly all our [100] tilt boundaries have perfect planar matching of the (100) planes whereas the [110] boundaries contain matching (110) planes. Since it is evident that geometry alone does not determine boundary energy, as has already been pointed out (34), it may be that there is a particularly felicitous electronic matching across (100) planes which is independent of boundary inclination whereas across (110) this does not occur, allowing geometry to play a larger role.

4.3 <110> Tilt Boundaries

It has been shown recently that low angle (110) twist boundaries in gold adopt a hexagonal network of dislocations (35). This array is shown in Figure 12 with the $[\bar{1}11]_m$, $[1\bar{1}1]_m$ and $[001]_m$ directions indicated on it. Also indicated are the corresponding O-lattice elements (indicated by the x's and +'s) which in this case are generated by an inhomogeneous transformation between the two grains (35). The planes containing the highest density of O-lattice elements then lie along $[\bar{1}11]_m$, $[1\bar{1}1]_m$ and $[001]_m$ and are shown dashed in Figure 12. Boundaries lying along these directions should again by of relatively low energy since again they should possess a relatively low density of identical dislocations possessing elementary lattice Burgers vectors. In line with this expectation these three facets are indeed those observed most frequently in boundaries with misorientations up to 15^{o}. Actually the $[\bar{1}11]_m$ and $[1\bar{1}1]_m$ facets are observed continually up to $\theta\sim35^{o}$. However for high angle boundaries the discrete dislocation representation is physically unreasonable and we therefore proceed by considering the results on the basis of a CSL approach.

Several of the facets observed in boundaries of higher misorientation angle coincide with high density CSL planes. For example the $[01\bar{1}]_m$ in the $\theta= 50.5^{o}$ misorientation (Σ11) has a PCSD of 1.21, which is the highest density achieved by any CSL plane

except the coherent Σ3 twin. We observe faccts in the Σ11 boundaries which adopt $[011]_m$ and we also observe $[111]_m$ facets with a PCSD of 0.40 in the 20.1° (Σ33) misorientation. However a tabulation of all the possible CSLs with Σ<100 which can be obtained by rotation about <110> (Table 2) shows that there are many CSLs whose most dense plane has a PCSD which exceeds 0.4. Many of these (for example $\Sigma 19, \theta = 26.5^\circ$; $\Sigma 27, \theta = 31.6^\circ$; $\Sigma 59, \theta = 46^\circ$) do not give rise to facets on the dense CSL plane, as comparison with Table 1 will confirm, even though the PCSD may be as high as 0.92. Coincidence site density therefore seems not to be the only criterion governing the energy of each boundary plane. It is unwise to extend the PCSD argument to draw conclusions from the presence or absence of second and third sets of facets on CSL planes of lower PCSD than the maximum for each misorientation since the Wulff-Herring construction shows that not only cusp depth but boundary inclination controls the theoretical occurrence of facets. For example the third most densely populated CSL plane in the Σ3 system, despite having a PCSD of 0.67, should never give rise to a facet even if cusp depth is proportional to PCSD, as Figure 10 indicates. Despite this note of caution we would certainly expect, if PCSD is a major predictor of boundary energy, to find abundant faceting on the densest CSL plane of those systems where there is a large difference in PCSD between the most dense and second most dense CSL planes. Examples of such CSLs are the Σ3,11,19,27 and 59 quoted above wherein the value of $PCSD_{most}/PCSD_{second}$ is $2\sqrt{2}$. However, we in fact see faceting onto the highest PCSD plane in two of these systems (Σ3 and 11) but not in the other three, while on the other hand we see faceting onto the highest PCSD planes in both Σ33 misorientations when $PCSD_{most}/PCSD_{second}$ is only 1.15. We have also compared the observed facet planes with low index planes in a whole hierarchy of possible O-lattices in the <110> tilt system (see previous footnote on p 9). However, we could find no correlation between facet planes and O-lattice planes for high angle <110> boundaries.

We conclude from this discussion that in some cases a high angle grain boundary may facet onto a plane of a nearby CSL which has a relatively high PCSD. However we must recognize that other criteria also contribute to faceting since we find both:

a) high PCSD CSL planes on which no facet arises,

and b) faceting on planes which appear to have no particular significance in the CSL (e.g. at $\theta = 46^\circ$ and 62°).

4.4 Boundary Dissociation

The dissociation of a high angle grain boundary into a Σ3 twin and a third boundary is a frequent observation in [110] misoriented tilt boundaries. The geometry of our specimens clearly only permits such a dissociation because there is a Σ3 misorientation attainable by rotation of 70.53° about [110] and the coherent twin boundary is thus created perpendicular to the thin film, in its position of least area. In principle then any [110] boundary of misorientation θ could dissociate into Σ3 and X with misorientations ±70.5 and θ ∓70.5. However our observations indicate that this only happens when θ lies within certain ranges, presumably because only certain combinations of dissociated boundaries lower the total free energy. As far as our limited number of bicrystals enables us to determine, the only boundary misorientations which led to frequent dissociation were within a few degrees of Σ11, Σ9 and Σ99. In terms of both CSLs and misorientations the dissociations were thus:

Σ11	→ Σ3	-	Σ33	50.5° → 70.5° - 20.0°
Σ9	→ Σ3	-	Σ3	38.9° →109.4° - 70.5°
Σ99	→ Σ3	+	Σ33	90.5° → 70.5° + 20.0°

The Σ9 dissociation illustrated in Figure 8 is to be expected since the low energy of the coherent and incoherent facets of the Σ3 twin are well known. Indeed Vaughan (21) has previously reported similar triangular mutual twins at a Σ9 boundary in stainless steel, although he interpreted them as being trapped by the running together of two primary twins on different systems in the same grain. In our specimens the dissociation must be real. A further difference between our observations and Vaughan's is the habit plane of the incoherent twin boundary which is $\{112\}_1$ vs. $\{112\}_2$ in our gold specimens but was $\{\bar{7}\ 7\ 11\}_1$ vs. $\{5\ \bar{5}\ \overline{13}\}_2$ in the stainless steel. This is yet another piece of evidence that geometry is not the sole determinant of even relative boundary energies.

All the other boundary dissociations which we observed (e.g. Figures 7 & 9) involved a Σ33 boundary. There seems to be no geometric reason why this otherwise unremarkable boundary should have a particularly low energy but it has also been found to be of low energy in the sphere sintering experiments of Herrmann et al (36). Another unexplained feature is that so far we have

.../13.

not observed the dissociation of a boundary in the misorientation range 60-80° [110] into Σ3 plus a low angle boundary of relatively low energy. Possibly nucleation of the low angle boundary is the problem here rather than free energy reduction, although Chaudhari and Mader (37) have reported seeing small angle boundaries resulting from the dissociation of a 30° <111> boundary into Σ13 + 2° boundaries.

In our bicrystal specimens the actual mechanism of the dissociation of the high energy boundaries is complex and has not yet been observed dynamically (for example in a TEM hot stage). Some possible mechanisms have already been discussed by one of us (38). Basically the criterion for nucleation of twins is still the reduction of boundary free energy laid down by Fullman and Fisher (39) and subsequently confirmed and discussed for lead and copper by Aust and Rutter (40) and Viswanathan and Bauer (14).

Finally, it is noted that the present technique is complementary to the "sintering of spheres on a plate" method (34, 36) as a basic technique for studying relative grain boundary energies. In the present method the crystal misorientation is fixed, of course, and effects due to variation in the orientation of the grain boundary plane are observed. In the latter method the average orientation of the grain boundary plane is fixed (parallel to the single crystal plate) and the effects of variation in the crystal misorientation are observed.

5. CONCLUSIONS

a) Low angle tilt boundaries with misorientation axes <100> and <110> tend to facet onto boundary planes containing a high density of O-lattice elements of properly chosen O-lattices. Physically. this corresponds to low energy situations where the boundary consists of a low density of identical lattice dislocations lying at the spacing of the O-lattice and possessing elementary lattice Burgers vectors.

b) High angle <100> tilt boundaries in gold show no tendency to facet.

c) High angle <110> tilt boundaries in gold facet frequently. In many cases the facet plane is a CSL plane with a high density of coincident sites. In other cases the facet plane cannot be

.../14.

related to a CSL and it therefore appears that geometry is not the sole determinant of relative boundary plane energies.

d) <110> tilt boundaries near the $\Sigma 11$, $\Sigma 9$ and $\Sigma 99$ misorientations frequently dissociate giving a $\Sigma 3$ twin and a second boundary which is frequently a $\Sigma 33$ boundary which must therefore be of particularly low energy.

ACKNOWLEDGEMENTS

Much of the work reported in this paper was supported by the Energy Research and Development Administration under contract E(11-1)-2679. Additional support was received from the National Science Foundation through the Materials Science Center at Cornell University.

****

TABLE 1

FACETS OBSERVED IN BICRYSTALS MISORIENTED BY θ ABOUT [110]

θ ±1°	CSL (if within 2°)	Facets	Dissociation
2		$[1\bar{1}1]_m$ $[\bar{1}11]_m$ $[001]_m$	
8			
15	73 & 51		
20	33	$[1\bar{1}1]_m$ $[\bar{1}11]_m$	
22	51		
24	51		
28	19		
37	9		Yes
41	9		Yes
46	59	$\pm 65^\circ$ from $[001]_m$	
48	59 & 11		Yes
50	11	$\pm 30^\circ$ & $\pm 75^\circ$ from $[001]_m$	Yes
52	11	$[1\bar{1}0]_m$	Yes
59	33	$[1\bar{1}2]_m$ $[\bar{1}12]_m$ $[1\bar{1}0]_m$	
62	67	$\pm 22^\circ$ from $[001]_m$ $[1\bar{1}0]_m$	
64	67	$[001]_m$ $[1\bar{1}2]_m$ $[\bar{1}12]_m$	
70	3	$[1\bar{1}0]_m$ $[001]_m$	
90	99	$[1\bar{1}0]_m (= [001]_m)$ $[1\bar{1}1]_m$ $[\bar{1}11]_m$	Yes

TABLE 2

Densly packed CSL planes generated by rotations about [110]. The plane of highest PCSD in each CSL is indicated by the direction along which it intersects the (110) plane (the plane of our specimens).

Σ	θ	Densest CSL Plane	PCSD max.	Facet Seen ?
99	11.5	$[001]_m$	0.40	?
73	13.4	$[1\bar{1}1]_m$	0.27	Yes
51	16.1	$[001]_m$	0.56	?
33	20.1	$[1\bar{1}1]_m$	0.40	Yes
51	22.8	$[1\bar{1}0]_m$	0.56	No
19	26.5	$[001]_m$	0.92	No
27	31.6	$[1\bar{1}0]_m$	0.77	No
89	34.9	$[1\bar{1}2]_m$	0.17	
9	38.9	$[1\bar{1}1]_m$	0.77	Yes
57	44.0	$[1\bar{1}2]_m$	0.22	
59	46.0	$[001]_m$	0.52	No
11	50.5	$[1\bar{1}0]_m$	1.21	Yes
41	55.9	$[1\bar{1}1]_m$	0.36	
33	59.0	$[1\bar{1}2]_m$	0.40	Yes
97	61.0	$[1\bar{1}1]_m$	0.17	No
67	62.4	$[1\bar{1}0]_m$	0.49	Yes
3	70.5	$[1\bar{1}0]_m$	2.31	Yes
81	77.9	$[1\bar{1}2]_m$	0.18	
43	80.6	$[1\bar{1}0]_m$	0.61	
57	83.0	$[1\bar{1}1]_m$	0.22	
17	86.6	$[1\bar{1}2]_m$	0.56	
99	89.4	$[1\bar{1}0]_m$	0.40	Yes

REFERENCES

1. H.Gleiter, Acta Met. 18 23 (70).

2a. E.W. Hart in Nature & Behaviour of Grain Boundaries, Ed.H.Hu 1972, p. 155.

2b. H.Gleiter, Z.Metallkunde 61 282 (70).

3. M.L. Kronberg and F.H. Wilson, Trans. AIMME 185 501 (49).

4. D.G. Brandon, B. Ralph, S. Ranganathan and M.S. Wald, Acta Met. 12 813 (64).

5. S. Ranganathan,Acta Cryst. 21 197 (66).

6. R.W. Balluffi & T.Y. Tan, Scripta Met. 6 1033 (72).

7. G.H. Bishop and B. Chalmers, Scripta Met. 2 133 (68).

8. H. Gleiter, Phys.Stat.Sol.b. 45 9 (71).

9. P.H. Pumphrey, Scripta Met. 6 107 (72).

10. B. Ralph, P.R. Howell and T.F. Page, Phys.Stat.Sol.b. 55 641 (73).

11. G.H. Bishop, W.H. Hartt and G.A. Bruggeman, Acta Met. 19 37 (71) & Ibid 22 971 (74).

12. M.J. Weins and J.J. Weins, Phil.Mag. 885 (72).

13. W.R. Wagner, T.Y. Tan and R.W. Balluffi, Phil.Mag. 29 895 (74).

14. R. Vishwanathan and C.L. Bauer, Met.Trans. 4 2645 (73).

15. A. Donald, Phil.Mag. 34 1185 (76).

16. J.W. Matthews, Phil.Mag. 7 915 (62).

17. R.L. Fullman, J.Appl.Phys. 22 456 (51).

18. C.M. Sargent, Trans. AIMME 242 1188 (68).

19. R.C. Pond, J.de Physique C4, 36 315 (75).

20. S. Dash and N. Brown, Acta Met. 111067 (63).

21. D. Vaughan, Phil.Mag. 22 1003 (70).

22. D. Whitwham, M. Mouflard and P. Lacombe, Trans. AIMME 191 1070 (51).

23. P.L. Bolin, R.J. Bayuzick and B.N. Ranganathan, Phil.Mag. 32 891 (75).

24. T. Schober and R.W. Balluffi, Phil.Mag. 20 511 (69).

25. R.W. Balluffi, P.J. Goodhew, T.Y. Tan and W.R. Wagner, J. de Physique C4 36 17 (75).

26. R.M. Allen and P.J. Goodhew, Acta Met. In press.

27. G. Wulff, Z.Kristallog. 34 449 (01).

28. C. Herring, Phys.Rev. 82 87 (51).

29. P. Chaudhari and S. Mader in discussion after G. Hasson et al Surf.Sci. 31 115 (72).

30. M.C. Inman and H.R. Tipler, Met. Reviews 8 105 (63).

31. L.E. Murr, Scripta Meta. 6 203 (72).

32. S.L. Sass, T.Y. Tan and R.W. Balluffi, Phil.Mag. 31 559 (75).

33. J.M.C.Li J.Appl.Phys. 32 525 (61).

34. G. Herrmann, H. Sautter, G. Baro and H. Gleiter, Proc. 4th Bolton Landing Conference 'Grain Boundaries in Engineering Materials' Ed. J.L. Walter, J.H. Westbrook and D.A. Woodford (Claitors, Baton Rouge, 1974) p. 43.

35. P.J. Goodhew, T.P. Darby and R.W. Balluffi, Scripta Met. 10 495 (76).

36. G. Herrmann, H. Gleiter and G. Baro, Acta Met. 24 353 (76).

37. P. Chaudhari and S. Mader, Appl. Phys. Letters 20 483 (72).

38. P.J. Goodhew, Proc. Jersey Conf. 'Grain Boundaries' 1976 p A40.

39. R.L. Fullman and J.C. Fisher, J.Appl.Phys. 22 1350 (51).

40. K.T. Aust and J.W. Rutter, Trans. AIMME 218 1023 (60).

41. W. Bollmann "Crystal Defects and Crystalline Interfaces" Springer Verlag. N.Y. 1970.

****

FIGURE CAPTIONS

FIGURE 1 The geometry of the thin film specimens. The original twist boundary (a) migrates on annealing (b) to create tilt boundaries perpendicular to the film (c). The resultant island grains may facet or suffer boundary dissociation (d).

FIGURE 2 Islands showing strong faceting in the $\Sigma 3$ system.

FIGURE 3 Faceted {112} twin boundaries in a quadruply positioned {111} film.

FIGURE 4 One quadrant of a polar histogram showing the distribution of inclinations of 7.5^{o} [100] tilt boundaries. The radial distance from the origin is proportional to the length of boundary in that inclination.

FIGURE 5 A faceted island grain in the $\Sigma 11$ system (50.5^{o} [110]).

FIGURE 6 Faceted boundaries symmetrically disposed about $[1\bar{1}0]_m$ in the 47.5^{o} [110] system.

FIGURE 7 Twins within island grains in the $\Sigma 11$ (50.5^{o} [110]) system.

FIGURE 8 The dissociation of a $\Sigma 9$ (38.9^{o} [110]) boundary into triangular segments bounded by first order twins.

FIGURE 9 The dissociation of a 89^{o} [110] boundary ($\sim\Sigma 99$) into some segments bounded by first order twins.

FIGURE 10. The Wulff-Herring construction to determine the equilibrium shape of island grains in the Σ3 system. The assumed energy values are discussed in the text.

FIGURE 11 A wulff-Herring plot for the Σ5 system (36.9^{o} [100]).

FIGURE 12 The dislocation network and O-rods in a low angle [110] twist boundary.

****

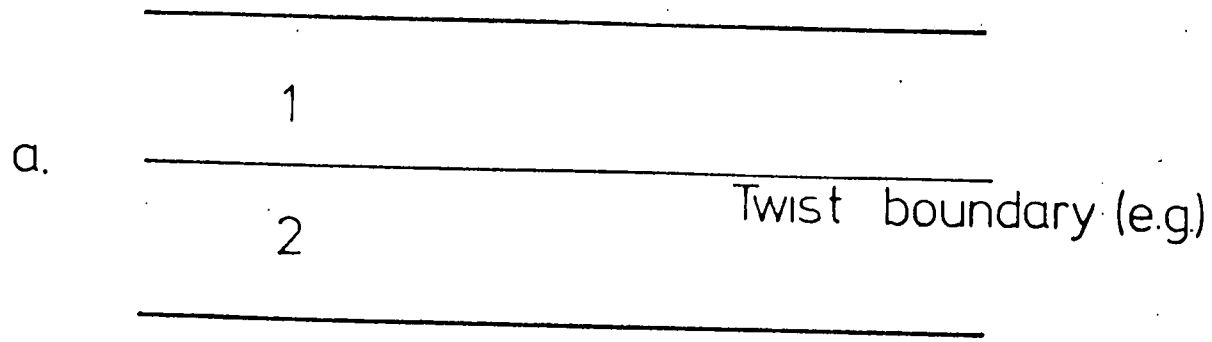
a.
1
2
Twist boundary (e.g.)

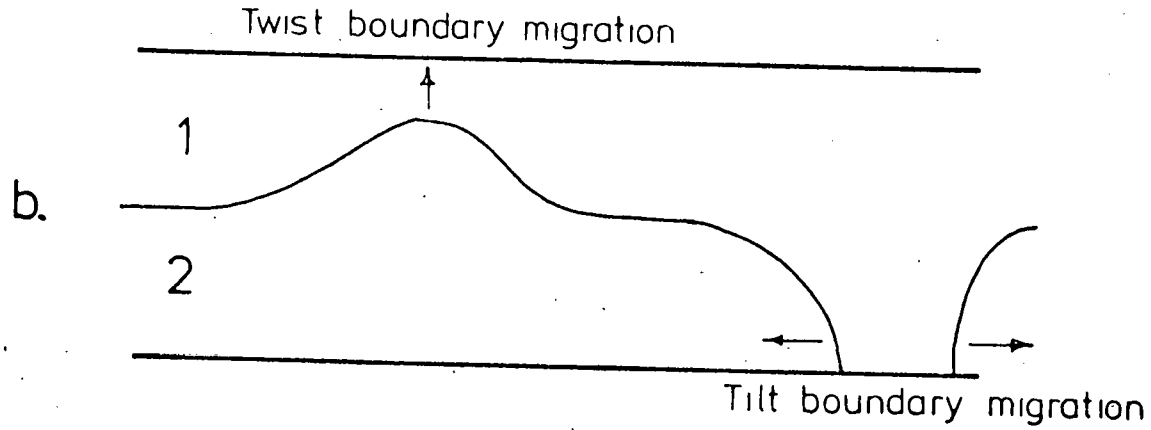
Twist boundary migration
b.
1
2
Tilt boundary migration

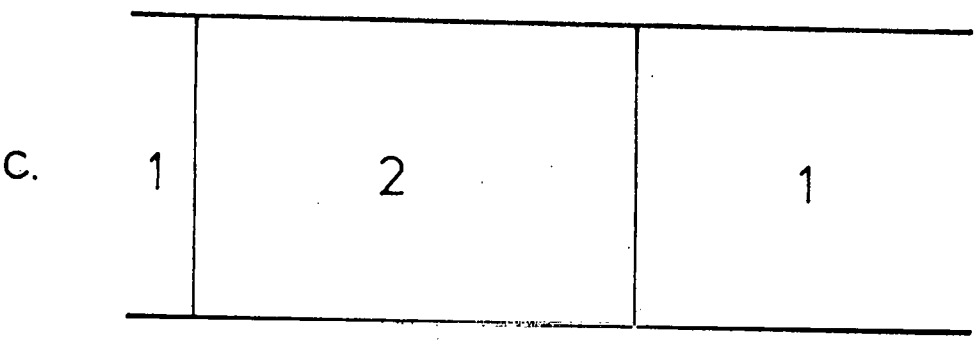
c.
1
2
1

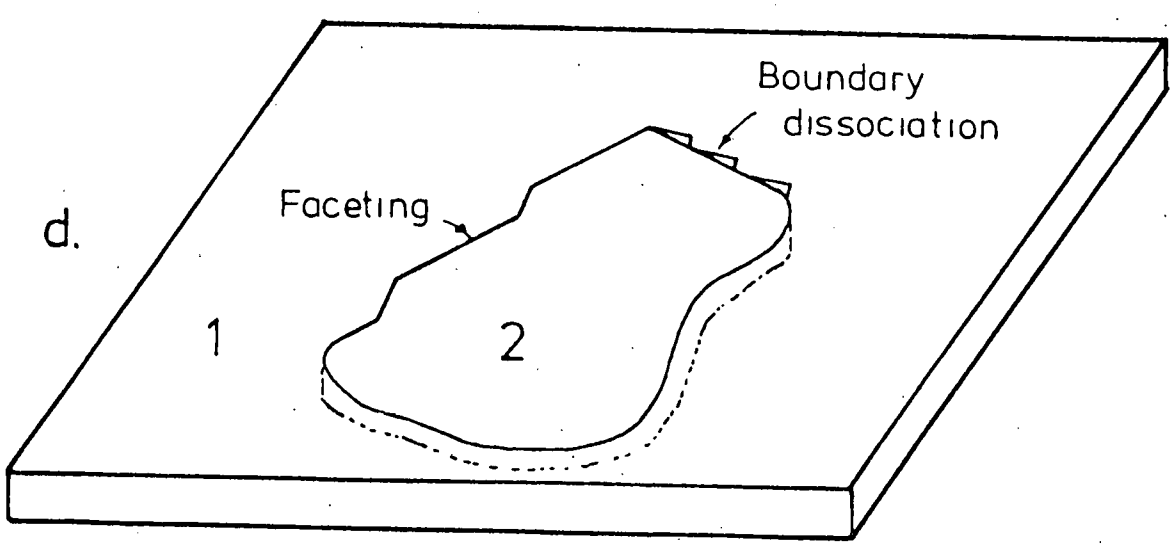
d.
Boundary dissociation
Faceting
1
2

Fig. 1

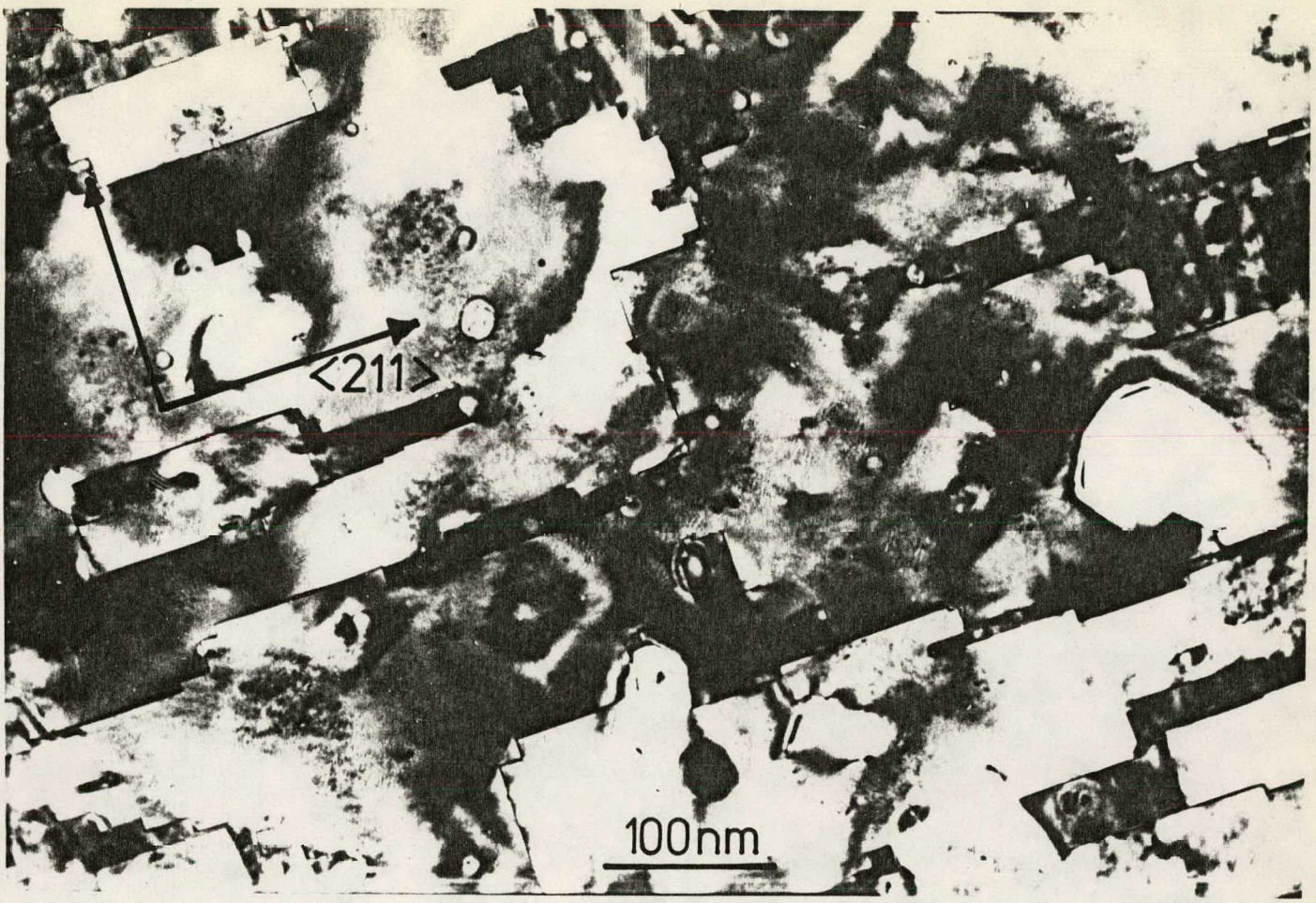

Fig 2

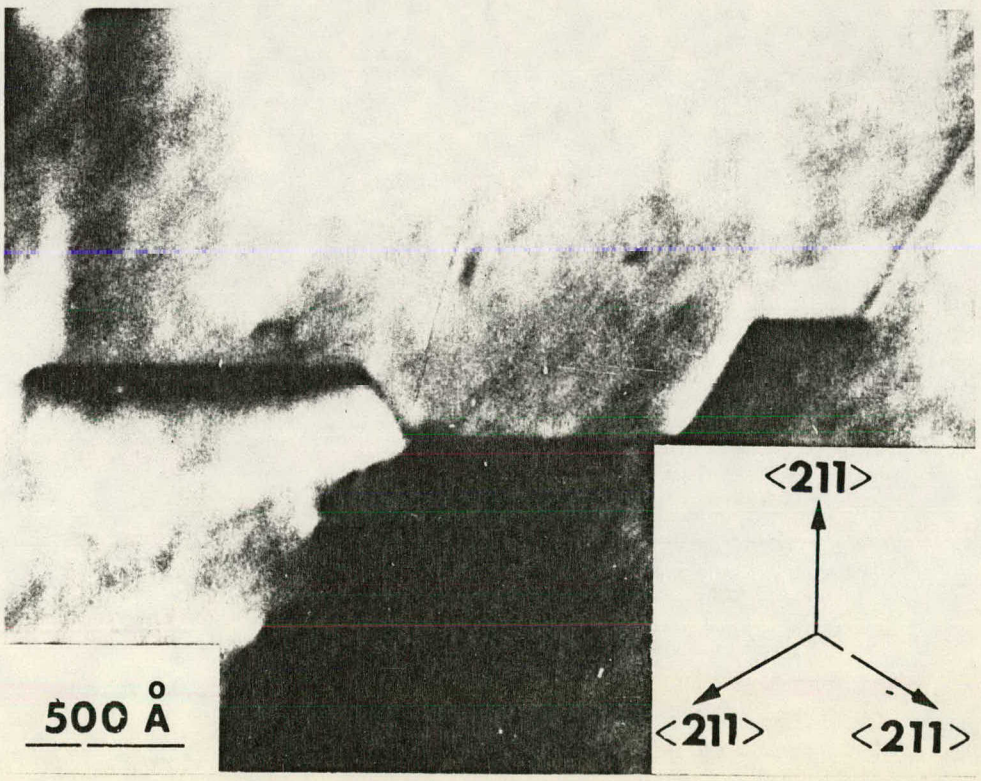

Fig 3

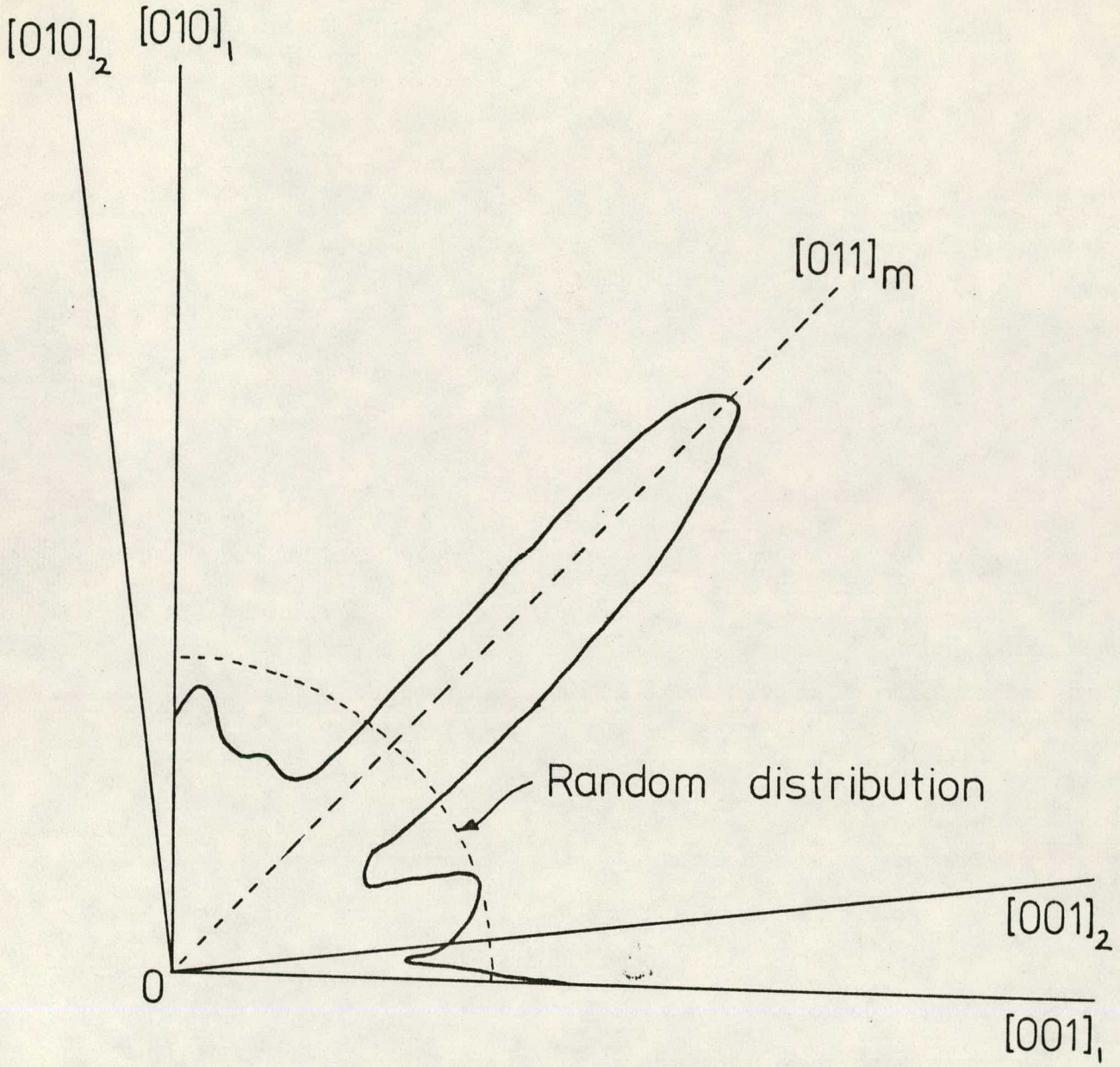

Fig 4

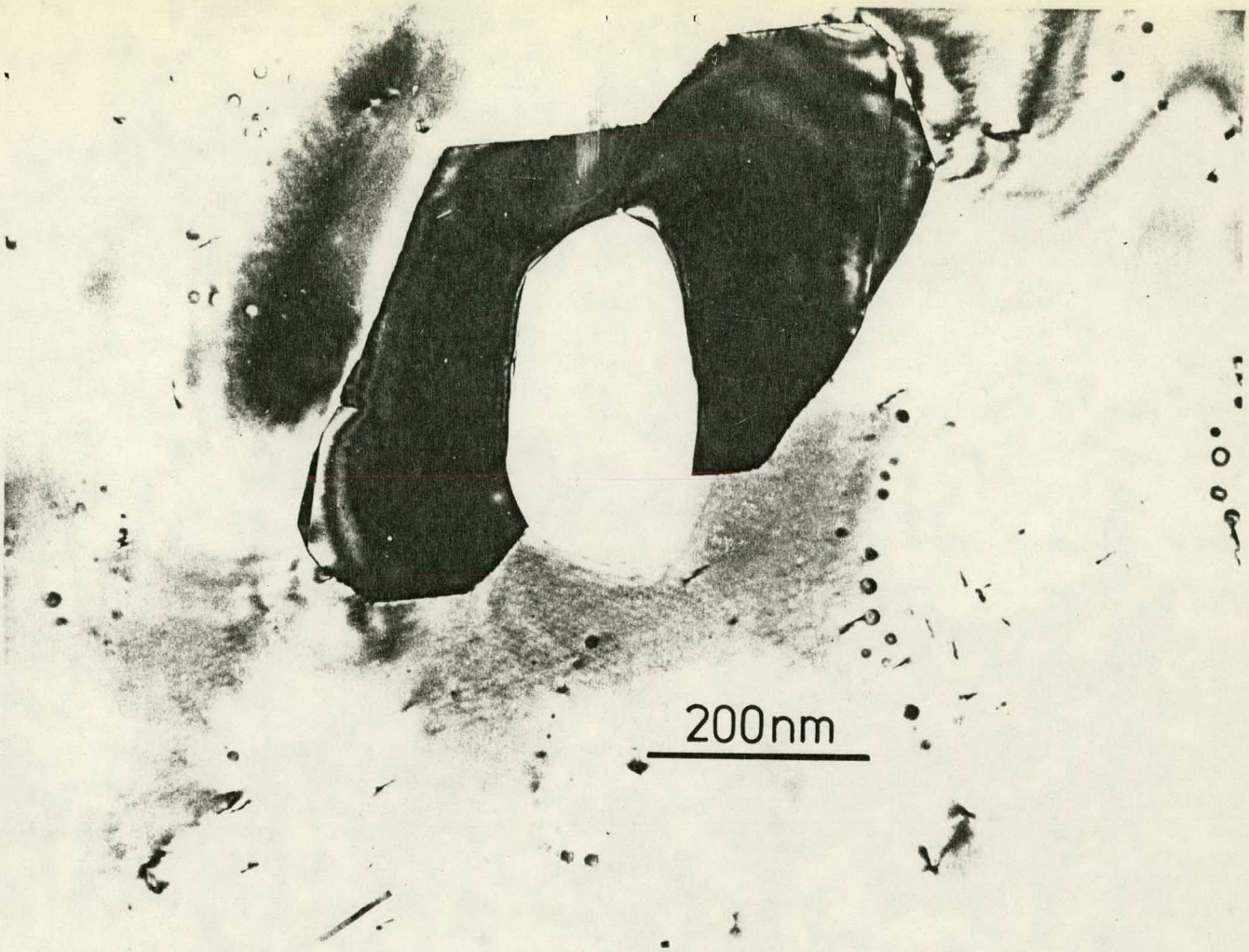

Fig 5

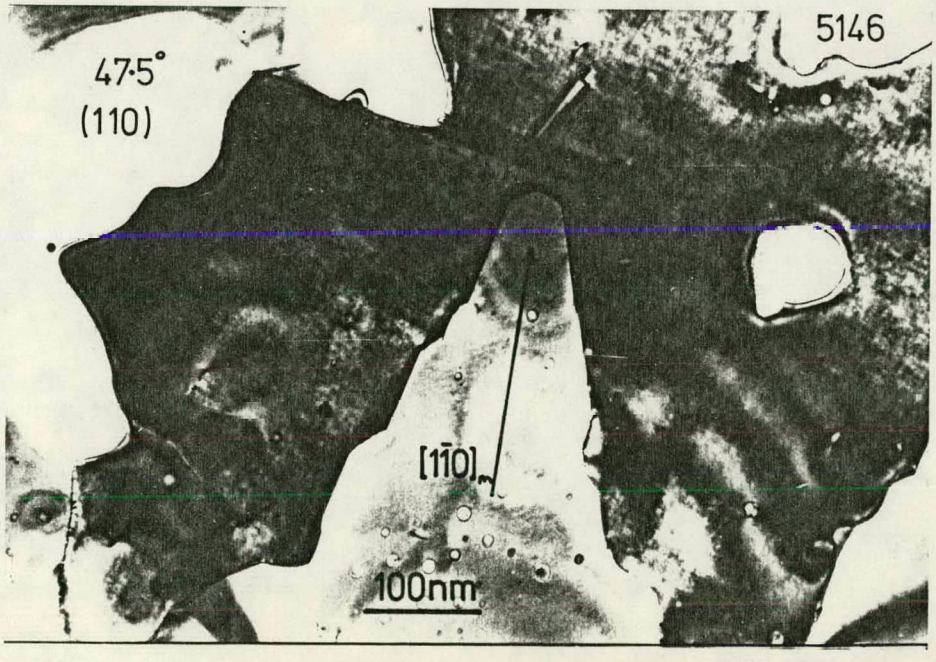

Fig 6

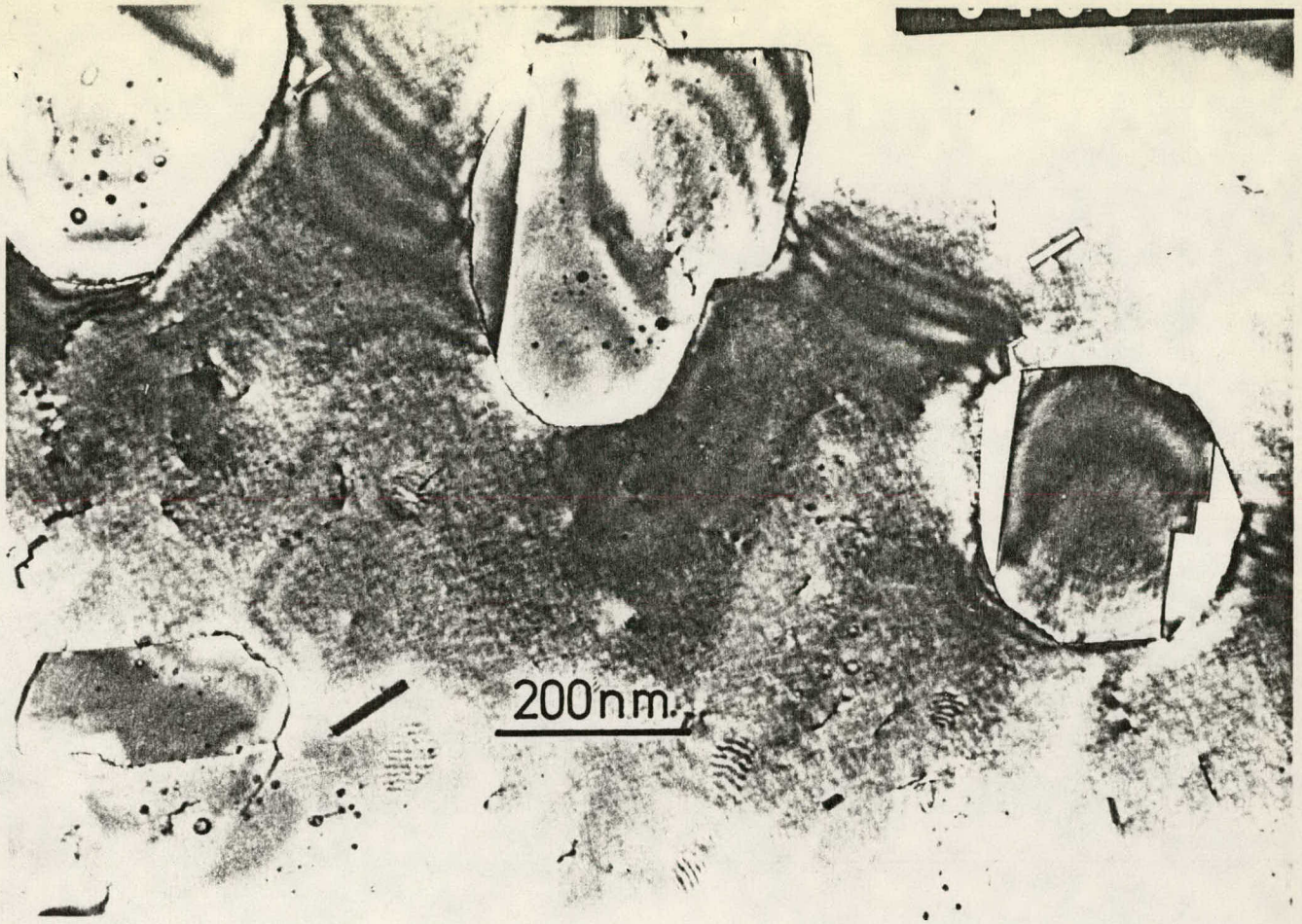

Fig 7

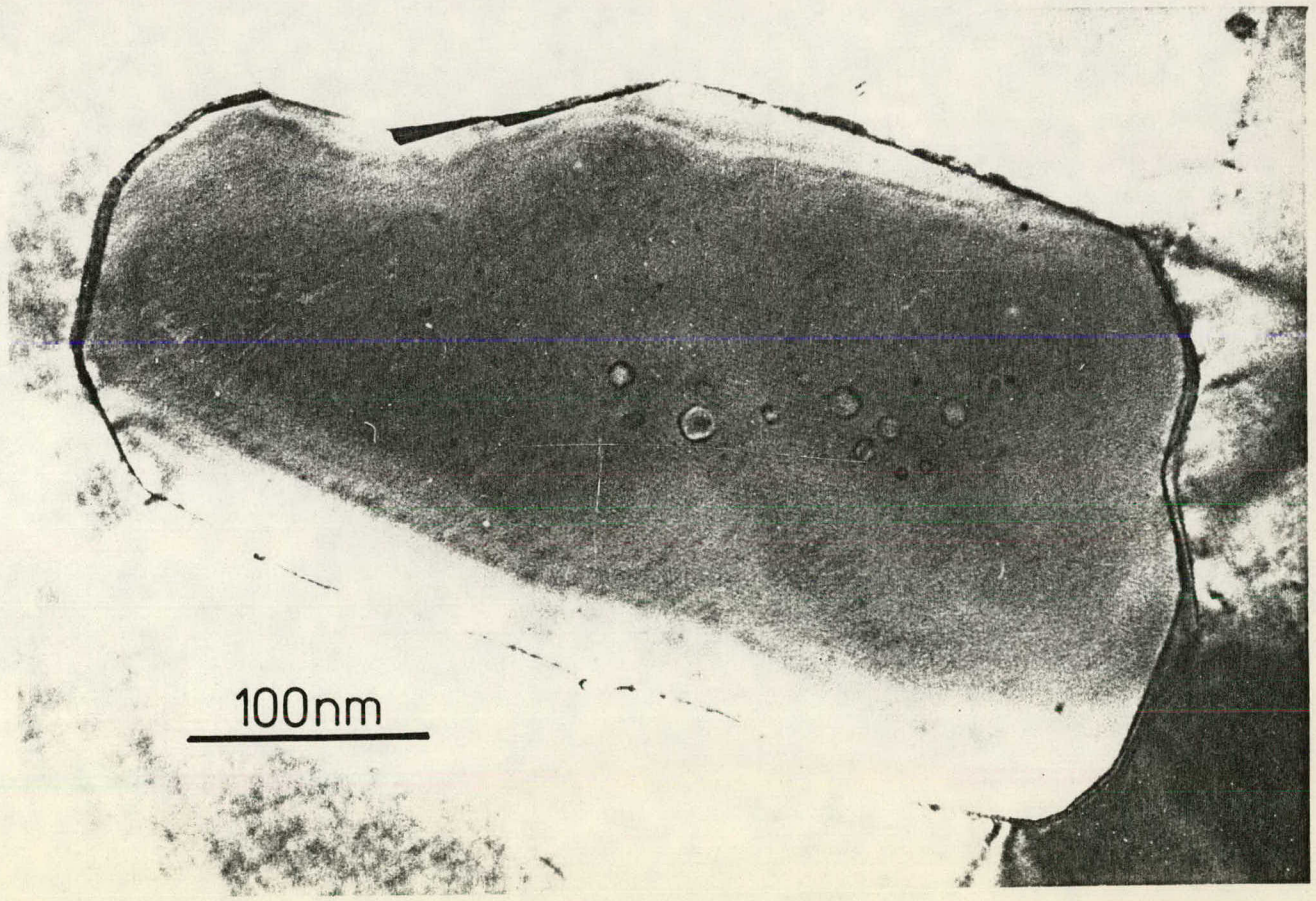

Fig 9

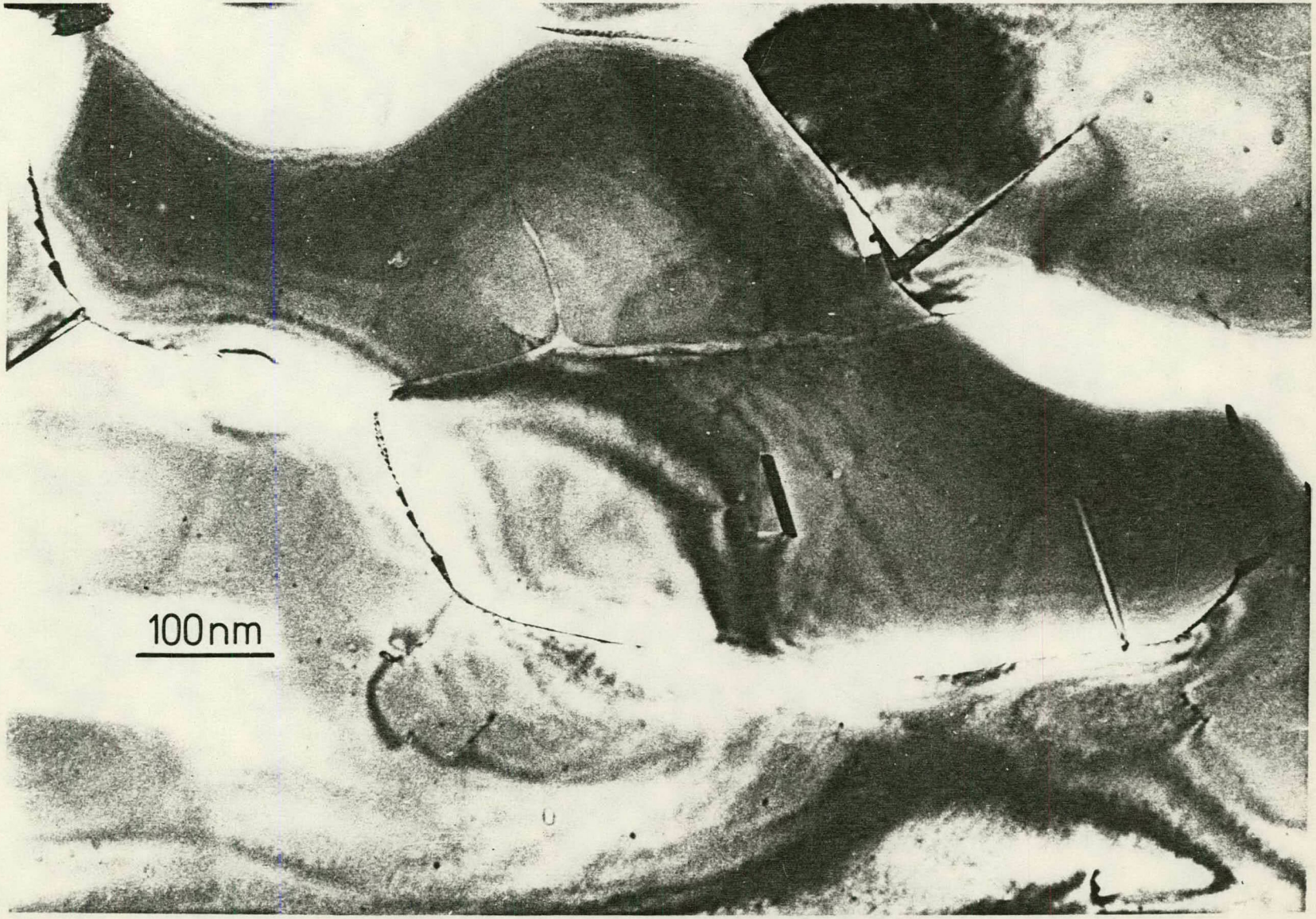

Fig 8

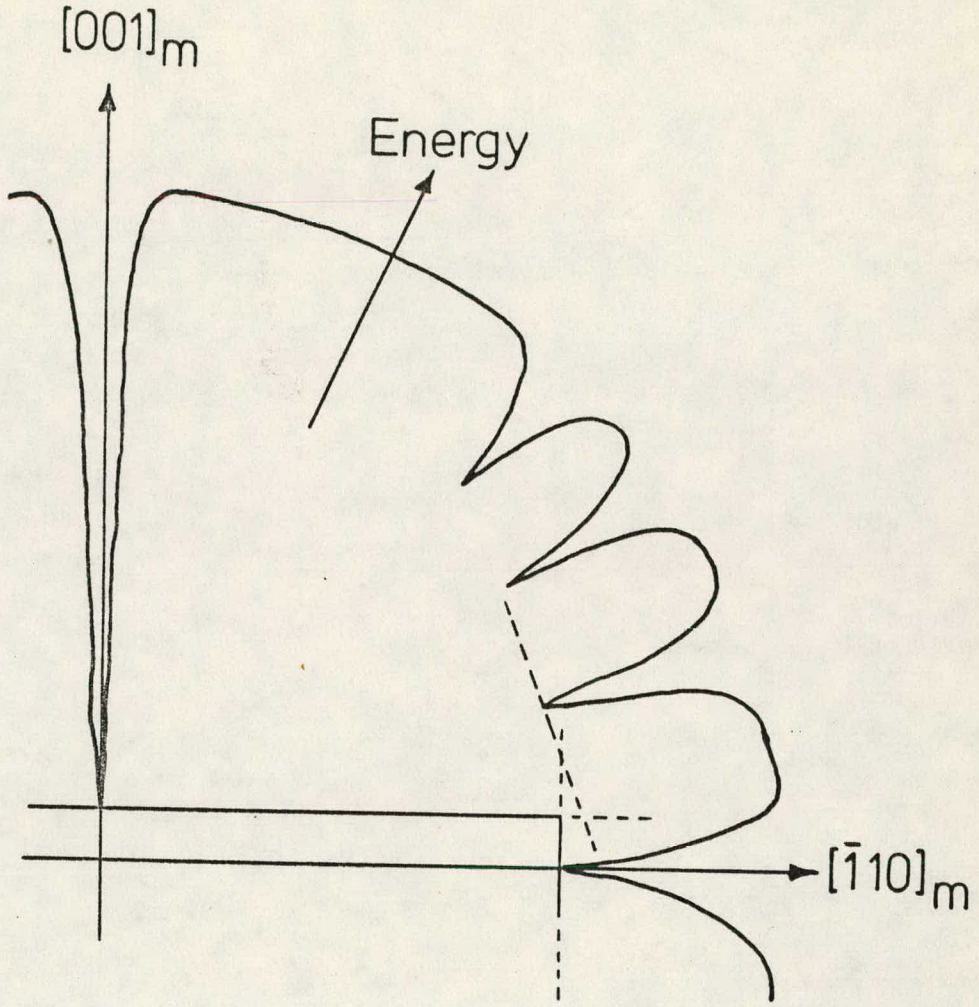

Fig 10

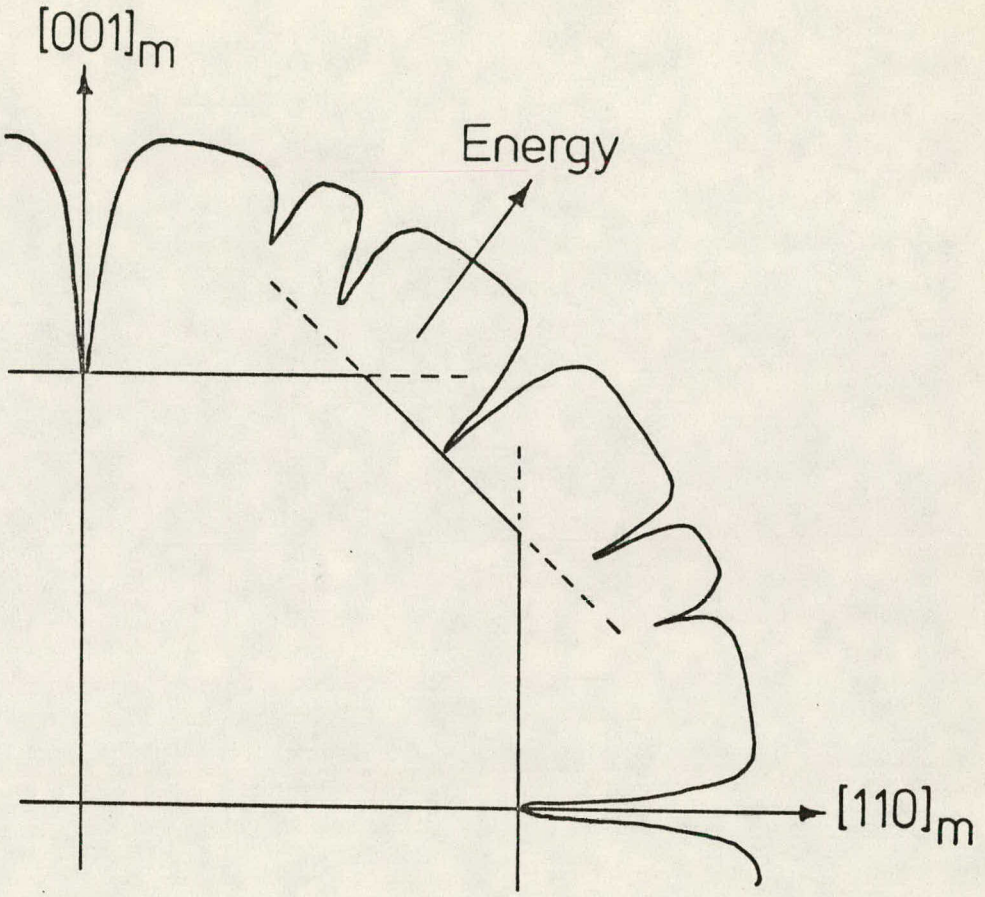

Fig 11

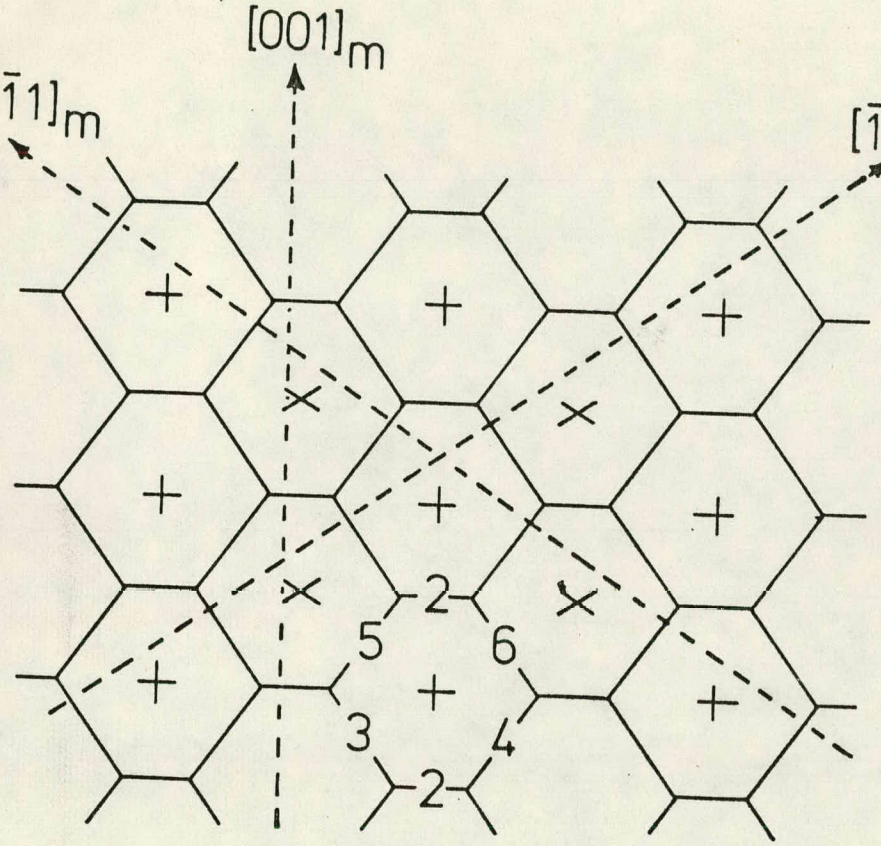

$$\vec{b}_2 = \frac{1}{2}[\bar{1}10]$$
$$\vec{b}_3 = \frac{1}{2}[101]$$
$$\vec{b}_4 = \frac{1}{2}[\bar{1}01]$$
$$\vec{b}_5 = \frac{1}{2}[011]$$
$$\vec{b}_6 = \frac{1}{2}[0\bar{1}1]$$

Fig 12